Proceedings of 14th IOE Graduate Conference
Peer Reviewed
Year: 2023 Month: December Volume: 14
ISSN: 2350-8914 (Online), 2350-8906 (Print)

Validation of the Z-Axis Deformation in Metal Plate during Welding: a Finite Element Approach

Kobid Kunwar [a], Jagat Kumar Shrestha [b], Arun Paudel [c]

[a] *Department of Civil Engineering, Pulchowk Campus, IOE, Tribhuvan University, Nepal*
[a] 078msste006.kobid@pcampus.edu.np, [b] jagatshrestha@ioe.edu.np, [c] arun.paudel@pcampus.edu.np

Abstract
This paper delves into a relatively under-explored area of research in Nepal, focusing on the thermal-induced structural behavior of construction elements. Welding-induced distortion is a critical issue in the construction industry, necessitating correction during assembly. To address this problem, the paper employs finite element analysis using FEM software - Ansys 2020. It conducts both transient thermal and transient structural analyses, considering temperature changes, conduction, and convection effects caused by a moving heat source. Material non-linearity is factored in, particularly in regions close to the heat source, to provide an accurate representation of the welding process. The central goal is to Prepare a Numerical model which closely predicts the deformation level of a subject element along z direction caused due to welding.

Keywords
Welding distortion, Thermal analysis, Structural analysis

1. Introduction

Welding is a foundational process in manufacturing and construction, vital for joining materials in various industries. It involves heating metals and often adding filler material to create strong assemblies. While welding has ancient origins, modern technology has led to diverse welding methods tailored for specific applications. Computational tools and finite element analysis have revolutionized welding by enabling virtual simulations. These simulations provide insights into temperature distribution, residual stress, and deformation, aiding in parameter optimization and improving weld quality while minimizing distortion. Welding continues to advance, addressing challenges like joining dissimilar materials and achieving high-performance welds in extreme conditions. This multidisciplinary field at the intersection of metallurgy, heat transfer, and mechanical behavior drives innovation, contributing to safer and more efficient designs across industries.

2. Literature Review

Different approaches for the prediction of distortion created during the fillet welding has been done before. The welding induced distortion has a history of more than five decades. Researchers like Rykalin and Vinokurov created analytical formulas for thermal field and welding deformation in the 1950s and 1960s using idealized geometry and heat source models [1]. Finite element techniques have been used to address welding thermal mechanical issues since the late 1970s [1].

2.1 Problems due to distortion

A further after-treatment operation, such as rectification, is needed because the welding distortion in a welded structure alters the structure's dimensions or makes the assembly process challenging [2]. Transverse and longitudinal distortion can lead to warping and buckling of thin sections, plates, or sheets, making it challenging to achieve flatness and causing difficulties in subsequent machining or processing steps. At the steel fabrication site, efforts are frequently undertaken using a number of ways to straighten the out-of-plane deformation that develops during actual welding of steel structures. The general consensus is that these operations not only slow down welding production by increasing the time required for fabrication and impeding the use of automated production systems, but they also negatively impact the strength of the structures being fabricated either directly or indirectly [2].

2.2 Welding-caused distortion: Quantification

2.2.1 Experimental Approach

Hui Huang and Ninshu ma has measured three deformation components, including longitudinal shrinkage, transverse shrinkage, and angular distortion after welding in an experiment [1]. In the experimental study conducted by Ninshu ma, two standard fillet welded connections with various cross sectional geometrical profiles are first carried out, after which welded structures with two parallel stiffeners and two stiffeners on both the longitudinal and transverse axes as a cross form are prepared and welding induced out-of-plane distortion is measured [3].

2.2.2 Analytical Approach

Shibahara and Ikushima, In their paper, a new analytical technique based on dynamic explicit FEM is proposed. Large time increments are possible with this technique to solve welding challenges. The suggested approach characterizes the welding events as quasi-static and disregards the effects of mass and damping. This indicates that the suggested method satisfies the model's static equilibrium criterion at each load stage [4]. The shipbuilding industry and other related production sectors are very concerned about the issues of distortion, residual stresses, and lower structural strength in and around a welded connection. The theoretical analysis of transverse shrinkage in a welded butt joint is the topic offered by Mandal and Sundar. In the study, thermo-elastoplastic zone and the totally elastic zone make up the plate that is being welded, according to the mathematical model that was employed for this investigation. The analysis offers a straightforward method for calculating welding shrinkage [5].

2.2.3 Numerical Modeling Approach

Deng and Kiyoshima performed simulation using mathematics of the welding temperature field, residual stress, and deformation due to electro slag welding. In this work, a computational method was created based on Quick Welder software to calculate the temperature field, residual stress distribution, and distortion caused by the ESW process. A 3-D finite element model with a moving heat source was used to perform a transient nonlinear heat transfer analysis under the stated welding conditions [6]. A three-dimensional numerical heat transfer and fluid flow model was created for the current work in order to investigate the temperature profiles, velocity fields, weld pool size and form, and the geometry of the solidified weld bead. Using a boundary fitted curvilinear coordinate system, the model was able to solve the equations of conservation of mass, momentum, and energy. The welding problem is assumed to be in steady state by employing a coordinate system that moves with the heat source. In other words, the material enters and exits the computational domain at the speed of welding while the heat source remains stationary in space. The momentum conservation equation that follows represents the movement of liquid metal in the weld pool [7].

3. Methodology

3.1 Preparation of Numerical model

Ansys 2020 has been used for the preparation of Finite Element Model. The modeling technique incorporates material properties of the base material, their characteristics of change in properties with respect to varying temperature; Geometry which involves selection of fundamental elements, meshing technique and its refinement, adoption of interface element; heat source modeling; thermal and structural boundary conditions; transient thermal analysis followed by transient structural analysis.

3.1.1 Nonlinear Thermal properties

The initial temperature distribution needs to be supplied for a transient thermal analysis. For a transient thermal analysis, thermal conductivity, density, and specific heat must be established [8]. The equations which should be taken into account for the determination of temperature distribution are transient non-linear heat transfer analysis, equation of volumetric flux and heat loss due to convection [6]. The thermal properties which are incorporated into the FE model are thermal conductivity(k) and specific heat(c). The varying values for those properties for different temperature data is given in the table below:

Table 1: Temperature dependent thermal properties [9]

Temperature (°C)	Thermal Conductivity, k (W/m.K)	Specific heat (J/Kg.K)
0	51.9	450
100	51.1	499.2
300	46.1	565.5
450	41.05	630.5
550	37.5	705.5
600	35.6	773.3
720	30.64	1080.4
800	26	931
1450	29.45	437.93
1510	29.7	400
1580	29.7	735.25
3500	42.1	400

3.1.2 Nonlinear Structural properties

For transient structural analysis which takes temperature as a thermal load, the material properties that should be defined are: Young's modulus, Poisson's ratio, coefficient of thermal expansion and density [8]. The adopted values for those properties for different temperature are given in the table below:

Table 2: Temperature dependent structural properties [9]

Temp (°C)	$\alpha(10^{-6}/°C)$	E (GPa)	ν
0	10	200	0.2786
100	11	200	0.3095
300	12	200	0.331
450	13	150	0.338
550	14	110	0.3575
600	14	88	0.3738
720	14	20	0.3738
800	14	20	0.4238
1450	15	2	0.4738
1510	15	0.2	0.499
1580	15	0.00002	0.499
3500	15.5	0.00002	0.499

3.1.3 Geometry

Geometry shown in Figure 1 is prepared using Autodesk revit 2021 and then imported in Ansys workbench.

Since, the ten-node tetrahedron has a strain field linear in coordinates, it represents fields of pure bending exactly [10], linear strain tetrahedral is taken as the basis element in highly affected elastoplastic regions where as eight node trilinear hexahedron is taken as the fundamental element for rest of the regions due to the computational convenience.

3.2 Meshing and Contact element

Due to the moving heat source, the region nearer to the flux is highly affected due to the high temperature. Heat affected zone (HAZ), which exhibits strongly non-linear behavior, should be

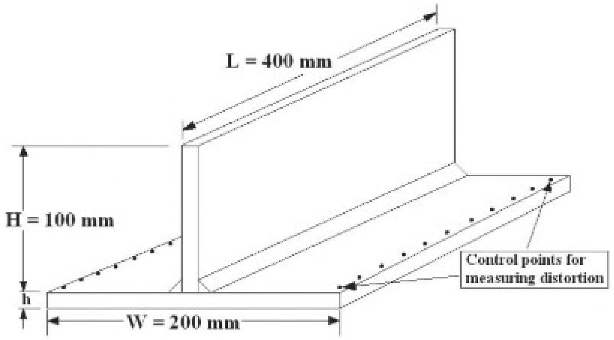

Figure 1: Plate dimension

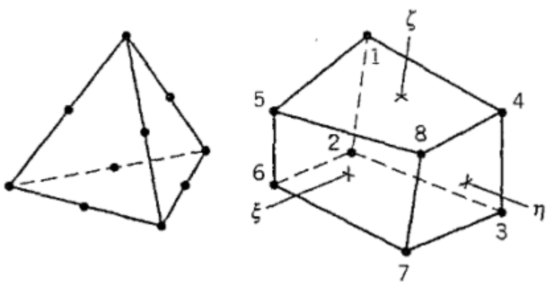

Figure 2: Fundamental Element

meshed with finer element and a comparatively coarser mesh can be applied to the less affected regions. Element size of 5 mm is input for the initial mesh generation.

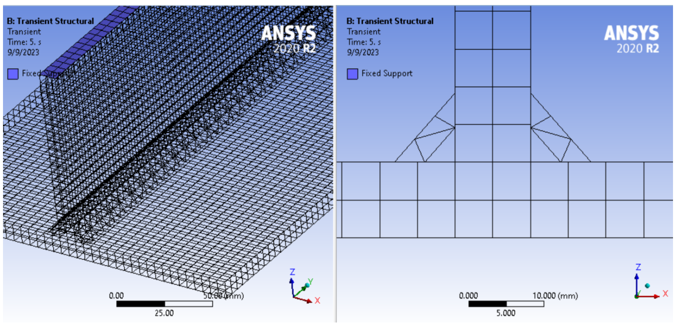

Figure 3: Meshing

Since, contact region is assumed to have no sliding and separation between faces or edges, bonded contact is modeled. Any gaps will be filled in and any initial penetration will be disregarded if contact is calculated based on the mathematical model [8].

3.3 Heat Source Model

During welding process, a continuous heat flux source is moved along the direction of welding. Energy per unit time per unit area is the definition of heat flux [8]. For the modeling of moving heat source, Gaussian distribution is adopted for the generation of the heat flux governed by the following equation throughout the course of application.

$$q = C_2 e^{\frac{[(x-x_0)^2+(y-y_0)^2+(z-z_0)^2]}{C_1^2}}$$

Where, C1 = radius of the beam; C2 = Heat source intessity = Power/Area of beam; xo, yo and zo = Illumination center point w.r.t. distance (time and speed); and q = Surface heat flux

Welding parameter adopted for the model are given in the table below:

Table 3: Welding parameter [9]

Current (A)	Voltage(V)	Welding Speed (mm/s)
470	27	5.0

3.4 Boundary Condition

Separate boundary conditions for thermal and structural analysis are defined to the model subjected to the thermal load.

3.4.1 Thermal Boundary Condition

Initial temperature and convection acts as a thermal boundary condition to execute thermal analysis. A transient thermal analysis includes time-varying loads. The initial temperature distribution at Time = 0 must be established before applying any transient thermal load [8]. Ansys uses those initial temperature distribution during first iteration of a transient thermal analysis [8].

Another boundary condition is convection. Convection causes convective heat transfer to occur through one or more flat or curved faces [8]. Ansys uses Newton's law of cooling for the convective heat transfer analysis.

3.4.2 Structural Boundary Condition

Temperature load distribution at each time step and support type acts as a boundary condition for the structural analysis of the model [8]. Temperature load after thermal analysis is imported as the the initial boundary condition by keeping in mind the source time step data feeds the exact same step of the analysis time. Another boundary condition for structural analysis is support type boundary condition. The support condition shown in the figure 4 is adopted for numerical modeling.

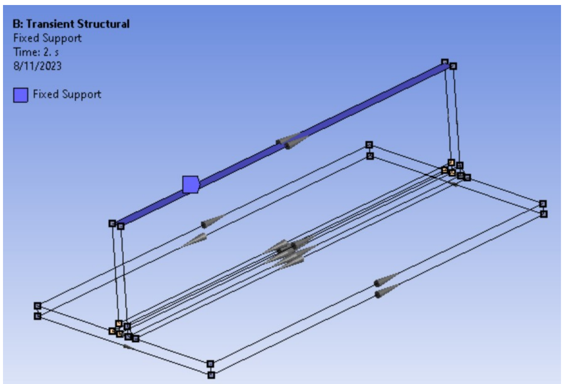

Figure 4: Support Condition

3.5 Analysis

The computed history of transient temperature profile is employed as a thermal loading and applied step by step for the further mechanical analysis. First, the temperature distribution at each time step is computed with heat transfer analysis and cooling down due to heat loss. Results for displacement, plastic strain, and residual stress can then be computed [3]. Welding-based distortion is directly related to the high temperature given during fusion, so a thermomechanical analysis i.e., thermal analysis subsequently followed by transient structural analysis has to be performed to encompass a true welding phenomenon [3].

3.5.1 Transient Nonlinear Thermal Analysis

Temperatures and other thermal parameters that change over time are determined through transient thermal studies [8]. The governing equation for investigations of transient nonlinear heat transfer is given as,

$$\lambda_x\left(\frac{\partial^2 T}{\partial x^2}\right)+\lambda_y\left(\frac{\partial^2 T}{\partial y^2}\right)+\lambda_z\left(\frac{\partial^2 T}{\partial z^2}\right)=\rho c\frac{\partial T}{\partial t}$$

[6]

3.5.2 Transient Structural Analysis

The solution of the thermal analysis is imported as a thermal load into the structural analysis, with the same time steps utilized in both analyses to ensure smooth continuity [9].

The formulations for stress-strain calculation used in the study are:

$$\sigma = \mathrm{D}\varepsilon^{\mathrm{e}}$$

Where,

$$\varepsilon^{\mathrm{e}} = \varepsilon - \varepsilon^{\mathrm{t}}$$

and

$$\varepsilon^{\mathrm{t}} = \Delta\mathrm{T}\begin{bmatrix} \alpha_{\mathrm{x}}\alpha_{\mathrm{y}}\alpha_{\mathrm{z}} & 0 & 0 & 0 \end{bmatrix}^{\mathrm{T}}$$

Where,

$\Delta\mathrm{T} = \mathrm{T_n} - \mathrm{T_a}$

$\mathrm{T_n}$ = Instant temperature at the point of interest

$\mathrm{T_a}$ = Ambient temperature

4. Results and Discussion

A comprehensive analysis was conducted utilizing Finite Element Analysis (FEA) software. The obtained results were combined with experimental data, yielding a comprehensive overview that integrates theoretical insights with real-world observations. This synthesis of numerical and experimental information serves to provide a comprehensive understanding of the studied phenomenon.

4.1 Comparison between Numerical and Experimental data

Figure 6 displays the temperature profile obtained from both experimental measurements and the numerical simulation of the Finite Element model over time at a specific test point labeled as "A," located 15 mm away from the vertical face of the test specimen. Experimental data is taken from the study conducted by Biswas, Mahapatra, and Mandal [9]. Initially, the graph rises as the heat source approaches the designated point "A." At time t = 40 sec, the test point reaches its maximum temperature, as evident in the graph, because the moving heat source is closest to the point where temperature measurements are taken. Subsequently, the temperature begins to decline as the heat source moves away from the test point.

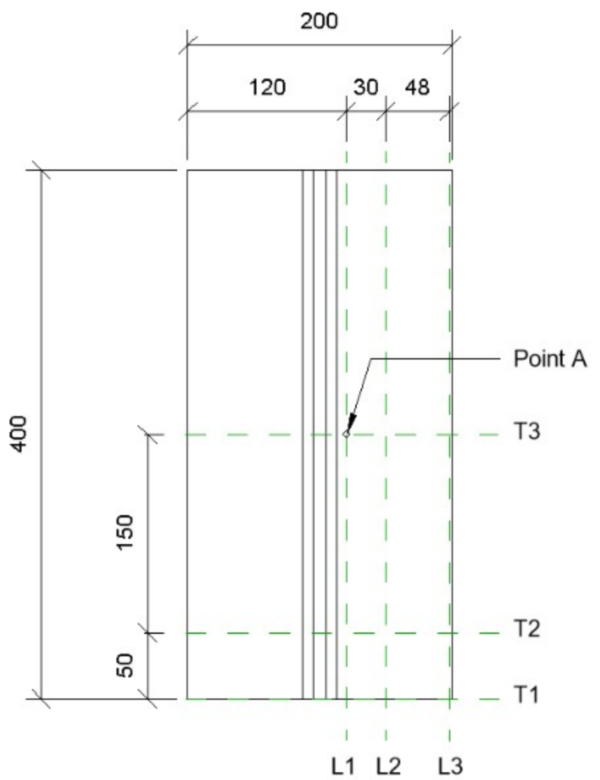

Figure 5: Test specimen showing reference points and lines

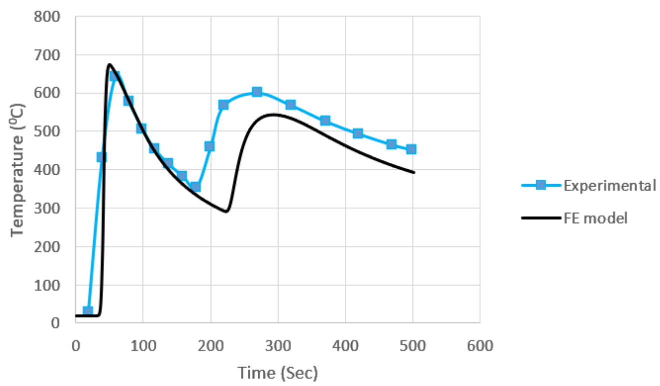

Figure 6: Temperature distribution at point A over time obtained from Experimental study and numerical modeling

A cooling period of 185 sec is provided before commencing welding on another face of the work-piece. At the conclusion of the cooling period, the curve once again ascends before gradually declining after passing the test point. Notably, during the second welding phase, the test point experiences a lower peak thermal value compared to the first welding phase. This is attributed to the fact that the heat source is slightly farther from the test point during the second welding phase.

Figures 7 and 8 show the Z-direction deformation along the right and left edges of the test specimen, respectively. Both graphs are convex upward, with the peak deformation occurring at their middle sections.

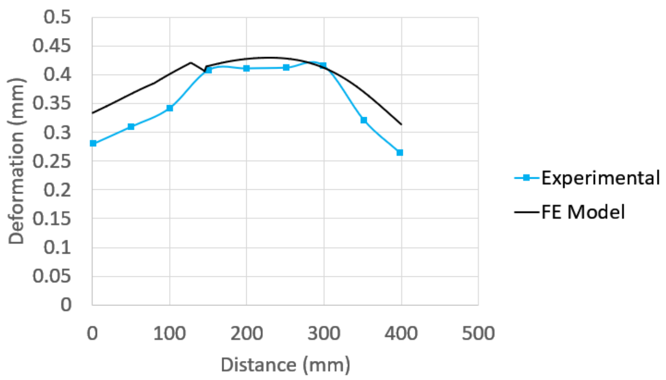

Figure 7: Distortion along Z axis at right face (at L3) of the test specimen

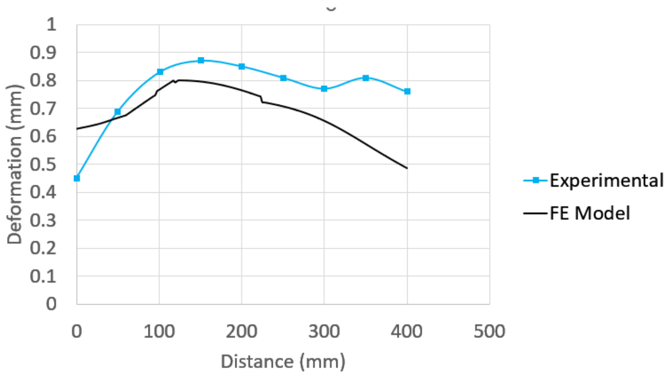

Figure 8: Distortion along Z axis at left face of the test specimen

5. Conclusion

The temperature profile obtained after the thermal analysis of the FE model matches the experimental data measured using a thermocouple. Hence, the model is validated for temperature distribution generated by the moving heat source.

Furthermore, the model is validated for z-axis deformation, as the deformations obtained after the mechanical analysis (conducted after the thermal analysis) closely match the deformations obtained experimentally using a Linear Variable Differential Transformer (LVDT).

References

[1] Hui Huang, Ninshu Ma, and Hidekazu Murakawa. Fast prediction of welding distortion using ISM and i-ISM with experimental validation. *Proceedings of the International Offshore and Polar Engineering Conference*, (April 2015):55–60, 2014.

[2] Sungwook Kang, Wangho Yun, Hwanjin Kim, Jaewoong Kim, Changwook Ji, Kwangjin Lee, Jaehwang Kim, Hong Lae Jang, and Kwangsan Chun. A study on minimizing welding deformation of joints for the sealing of emission after-treatment structure. *Materials*, 14(22):1–13, 2021.

[3] Ninshu Ma, Jiangchao Wang, and Yasuhisa Okumoto. Out-of-plane welding distortion prediction and mitigation in stiffened welded structures. *International Journal of Advanced Manufacturing Technology*, 84(5-8):1371–1389, 2016.

[4] Kazuki Shibahara, Masakazu; Ikushima. Osaka University Knowledge Archive : OUKA Development of analytical method for welding mechanics using idealized explicit FEM. 2010.

[5] N. R. Mandal and C. V.N. Sundar. Analysis of welding shrinkage. *Welding Journal (Miami, Fla)*, 76(12):233–s, 1997.

[6] Dean Deng and Shoichi Kiyoshima. Numerical simulation of welding temperature field, residual stress and deformation induced by electro slag welding. *Computational Materials Science*, 62(December):23–34, 2012.

[7] W. Zhang, C. H. Kim, and T. DebRoy. Heat and fluid flow in complex joints during gas metal arc welding - Part I: Numerical model of fillet welding. *Journal of Applied Physics*, 95(9):5210–5219, 2004.

[8] ANSYS Inc. Mechanical User's Guide. *ANSYS, Inc.*, 15317(July):1028, 2021.

[9] P. Biswas, M. M. Mahapatra, and N. R. Mandal. Numerical and experimental study on prediction of thermal history and residual deformation of double-sided fillet welding. *Proceedings of the Institution of Mechanical Engineers, Part B: Journal of Engineering Manufacture*, 224(1):125–134, jan 2010.

[10] Robert D. Cook. Finite Element Modeling For Stress Analysis - R. Cook (1995) WW.pdf.